TIDAL JET FLOWS NEAR INLETS

by

Ümit A. Ünlüata and Emin Özsoy*

ABSTRACT

Turbulent jets issuing from tidal inlets during the ebb flows are analyzed and the effects of bottom friction and one-dimensional depth variations are shown to change the jet behavior in a drastic way. Jets on a constant bottom with friction expand in an explosive manner. When the depth increases in the offshore direction, the expansion rate of the jet is greatly reduced. The analytical solutions are verified against field evidence and preliminary experiments.

INTRODUCTION

The turbulent mixing and the flow patterns in the immediate neighborhood of tidal inlets have significant contributions to the transport of sediments in coastal waters [3], the exchange and mixing of estuarine or lagoonal waters with those of the ocean [8] and small scale circulations on the continental shelf. This paper describes the hydrodynamics of the turbulent jet flow issuing from a tidal inlet during the ebbing period, neglecting any complexities that may arise due to the presence of waves, winds, ambient currents, density stratification and secondary flows. The frictional resistance of the bottom and one dimensional depth variations are taken into account and the hydrodynamic variables are solved analytically. The results are compared with field evidence and experiments.

THEORETICAL MODEL

Water ebbing from a tidal inlet into a semi-infinite ocean creates a turbulent jet flow as shown in figure 1. The resultant flow has been studied previously [4] by making use of the classical two-dimensional jet theory. In the present case, however, the effluent is retarded by the frictional resistance of the bottom as well as through turbulent mixing with the ambient waters and the jet also adjusts itself to the depth variations. Since the flow is essentially two dimensional, it is adequately described by the depth averaged shallow water continuity and

* Coastal and Oceanographic Engineering Laboratory, University of Florida, Gainesville, Florida 32611. Present address of the first author: Department of Marine Sciences, Middle East Technical University, Ankara, Turkey.

momentum equations which have been derived elsewhere [10].

In the present case, these equations are further simplified, since the flow is boundary layer type i.e. the lateral length and velocity scales are much smaller than the longitudinal ones. The temporal accelerations (unsteady terms) and the free surface gradients (pressure terms) in the shallow water equations can be dropped following an order of magnitude analysis in the near field of the inlet mouth. The bottom friction is taken to be quadratic in the local velocity [10]. Therefore, the approximate equations of motion are

$$\frac{\partial}{\partial x}(hu^2) + \frac{\partial}{\partial y}(huv) = -\frac{f}{8} u^2 + \frac{1}{\rho} \frac{\partial}{\partial y} F_{yx} \tag{1}$$

$$\frac{\partial}{\partial x}(hu) + \frac{\partial}{\partial y}(hv) = 0 \tag{2}$$

in which u and v are the depth averaged horizontal velocity components respectively in the x and y directions indicated in figure 1, f the Darcy-Weisbach type bottom friction coefficient, ρ the density of the fluid and F_{yx} the longitudinal component of the depth integrated turbulent shear stresses.

Assuming the velocity profiles shown in figure 1 to be self-similar and allowing only one dimensional depth variations h = h(x), equations (1) and (2) can be reduced to ordinary differential equations. To this end, the following velocity profiles are adopted [1,7]: in the Zone of Flow Establishment (ZOFE), $x < x_s$ (see figure 1),

$$\frac{u}{u_c} = \begin{cases} 0 & ; \quad |y| > b \\ (1 - \zeta_0^{1.5})^2 & ; \quad r < |y| < b \\ 1 & ; \quad 0 < |y| < r \end{cases} \quad , \quad \zeta_0 = \frac{|y| - r}{b - r} \tag{3}$$

and in the Zone of Established Flow (ZOEF), $x > x_s$,

$$\frac{u}{u_c} = \begin{cases} 0 & ; \quad |y| > b \\ (1 - \zeta^{1.5})^2 & ; \quad 0 < |y| < b \end{cases} \quad , \quad \zeta = \frac{|y|}{b} \tag{4}$$

where u_c, r and b are respectively the centerline velocity, the core width and the jet width as shown in figure 1. The velocity of entrainment v_e into the jet is assumed to be proportional to the centerline velocity u_c [6] such that $v_e = \alpha u_c$, where $\alpha \simeq 0.03$ [9]. Ordinary differential equations governing the core width r(x), width b(x) and the centerline velocity $u_c(x)$ can be obtained by making use of the velocity profiles given in equations (3) and (4) and integrating the equations (1) and (2) across the jet. Thus, (noting that the velocity u and the shear force F_{yx} vanish as $y \to b$) we obtain

$$\frac{d}{dx}(hb\, u_c^2\, \bar{I}_2) = -\frac{f}{8} b u_c^2\, \bar{I}_2 \tag{5}$$

$$\frac{d}{dx}(h\, b\, u_c\, \bar{I}_1) = \alpha h u_c \tag{6}$$

where $\bar{I}_1(x)$ and $\bar{I}_2(x)$ are functions defined by

$$\bar{I}_1 = \int_0^1 \left(\frac{u}{u_c}\right) d\left(\frac{y}{b}\right), \quad \bar{I}_2 = \int_0^1 \left(\frac{u}{u_c}\right)^2 d\left(\frac{y}{b}\right) \tag{7}$$

ANALYTICAL SOLUTIONS

The inlet mouth is modeled by a rectangular slot of width $2b_0$ and depth h_0 and the inlet velocity is taken to be u_0. Defining the normalized variables

$$\xi = \frac{x}{b_0}, \quad \mu = \frac{f b_0}{8 h_0}, \quad H = \frac{h}{h_0}, \quad R = \frac{r}{b_0}, \quad B = \frac{b}{b_0}, \quad U = \frac{u_c}{u_0} \tag{8}$$

the solution to equations (5) and (6) follows immediately. In the ZOFE, we set U = 1 and the unknowns to be solved for are R and B, whereas in the ZOEF solutions are sought for B and U, since R = 0 in this region. The analytical solutions are [9]:

In the ZOFE, $\xi < \xi_s (= x_s/b_0)$,

$$R(\xi) = \frac{I_1 J(\xi) - I_2 G(\xi)}{(I_1 - I_2) H(\xi)}, \quad B(\xi) = \frac{(1 - I_2) G(\xi) - (1 - I_1) J(\xi)}{(I_1 - I_2) H(\xi)} \tag{9}$$

and in the ZOEF, $\xi > \xi_s$,

$$B(\xi) = \frac{L(\xi)}{I_2 H(\xi) J(\xi)}, \quad U(\xi) = \frac{J(\xi)}{L^{\frac{1}{2}}(\xi)} \tag{10}$$

where $$J(\xi) = \exp -\mu \int_0^{\xi} \frac{d\xi'}{H(\xi')} \tag{11}$$

$$G(\xi) = \alpha \int_0^{\xi} H(\xi')\, d\xi' + 1 \tag{12}$$

$$L(\xi) = \frac{2\alpha I_2}{I_1} \int_{\xi_s}^{\xi} H(\xi') J(\xi') d\xi' + J^2(\xi_s) \tag{13}$$

and $I_1 = 0.450$ and $I_2 = 0.316$ are constants which are also equal to the values of the functions $\bar{I}_1$ and $\bar{I}_2$ in the ZOEF. The details of the solution can be found in reference [9].

Considering some special cases, these solutions are studied further

in the following.

BOTTOM FRICTIONAL JETS WITH CONSTANT DEPTH

The general solutions in equations (9) - (13) can be simplified considerably [9] by taking a constant depth defined by H = 1. After these simplifications it is observed from the solutions that the jet width grows and the centerline velocity decays exponentially for sufficiently large values of the offshore distance; as opposed to the linear growth of the classical two-dimensional turbulent jet in which the centerline velocity decays as $\xi^{-\frac{1}{2}}$, hence much slower. The solutions for the jet width B and the centerline velocity U are displayed in figure 2 where μ is kept as a parameter. With increasing values of $\mu = fb_0/8h_0$ (i.e. for inlets having larger bottom friction or a larger width to depth ratio) the jet loses its momentum faster and exhibits an explosive growth. It is also worth noting that the classical, two-dimensional jet solutions may be recovered from the present theory by taking $\mu = 0$.

The fast growth rate of the bottom frictional jet has actually been hinted at in a number of previous works. In their experiments on jets in rotating basins, Savage and Sobey [5], have found that due to ~~the~~ bottom friction jets in shallow waters exhibit faster spreading rates than jets in deep waters. Taylor and Dean [8] have also found an exponentially growing jet, although the rate of expansion in their solutions is only half of that given by the present theory because they have neglected the lateral entrainment and assumed a uniform velocity distribution across the jet. Borichansky and Mikhailov [2] have analyzed non-buoyant jets near river mouths in a tideless sea by modeling the lateral friction on the effluent through a quadratic term analogous to the bottom friction term in equation (1). They also found an exponential growth although they are led to erroneous results since the lateral entrainment is neglected and the integral momentum of the jet is assumed to be conserved, contrary to the present theory. In reality, river effluents exhibit a significantly different behavior due to their buoyant spreading, and have been relatively well documented (for example see reference [11]).

BOTTOM FRICTIONAL JETS ON A LINEARLY VARYING TOPOGRAPHY

In the case of linear depth variations, simple forms of the analytical solutions in equations (9)-(13) are still possible [9] by taking $H = 1 + \nu\xi$, where $\nu = mb_0/h_0$ is a slope parameter with m being the slope of the bottom. Salient features of the solutions, some of which are shown in figure 3, can then be observed from these analytic forms. In general, as the slope parameter ν increases (such that either the slope or the inlet width to depth ratio increases) the jet expansion rate decreases and therefore the bottom slope counteracts significantly the rapid expansion due to the friction. This fact has also been recognized by Borichansky and Mikhailov [2]. When $\mu = \nu$, such that the frictional and the slope effects are in balance, the jet expands linearly in the ZOEF. In the case of a linearly decreasing depth ($\nu < 0$), the centerline velocity goes to zero and the width increases infinitely near the intersection point of the bottom and the surface. When the bottom is frictionless ($\mu = 0$) the jet grows linearly for large distances offshore of the inlet.

ARBITRARY DEPTH VARIATIONS

The general solutions in equations (9)-(13) can be evaluated by using numerical quadrature when the depth varies in an arbitrary manner. A sample calculation is carried out for Jupiter Inlet, Florida, for which the prototype values of the inlet half-width and depth are taken to be $b_0 = 50$m and $h_0 = 3$m, respectively. The friction is selected as $f \simeq 0.02$, thus implying $\mu \simeq 0.04$. Laterally averaged depth data is used to represent the one-dimensional bottom variations. Data from an unusually clear aerial photograph of the jet at Jupiter Inlet (figure 4) is used for comparison. The jet width is obtained graphically [9] from this photograph (figure 5) and compared with the results in figure 6 indicating a satisfactory agreement. The jet obviously expands while passing over the shoals and contracts afterwards due to the steep bottom gradient in front of the shoals.

EXPERIMENTS

Experimental measurements and further field evidence seems to be invaluable to the verification of the analytical solutions and the various assumptions involved in the theory. For this purpose, preliminary measurements of the jet centerline velocity were made. The model used in the experiments consisted of an inlet constructed on a sloping bottom built in a basin as shown in figure 7. The inclined bottom preexisted in the model basin and had a slope of $m \simeq 0.025$. The inlet half-width and depth were $b_0 = 10$ cm and $h_0 = 5$cm, respectively. Thus, assuming a friction factor of $f = 0.02$ yields $\mu = 0.05$ and $\nu = 0.05$ as the values of the friction and slope parameters. Measurements obtained in five individual experiments demonstrate a fair agreement with the analytical solution as shown in figure 8. The importance of the bottom friction is also displayed in figure 8 since the analytical solution for a frictionless bottom ($\mu = 0$) differs significantly from the observed variation of the centerline velocity.

ACKNOWLEDGEMENTS

The present work has emerged from listening to Prof. Robert G. Dean on several occasions. The experiments were carried out by Howard Groger, a University of Florida student to whom we are grateful.

REFERENCES

1. Abramovich, B.N. The Theory of Turbulent Jets, MIT Press, Cambridge, Massachusetts, 1973.
2. Borichanskiĭ, L.S. and V.N. Mikhailov, Interaction of River and Sea Water in the Absence of Tides, in Scientific Problems of the Humid Tropical Zone Deltas and Their Implications, UNESCO, pp. 175-180., 1966
3. Dean, R.G. and T.L. Walton, Sediment Transport Processes in the Vicinity of Inlets with Special Reference to Sand Trapping, Estuarine Research, Academic Press, 1974.
4. French, J.L., Tidal Flow in Entrances, U.S. Army Corps of Engineers, Committee on Tidal Hydraulics, Technical Bulletin No. 3, 1960.

5. Savage, S.B. and R.J. Sobey, Horizontal Momentum Jets in Rotating Basins, J. Fluid Mech., vol. 71, pp. 755-768, 1975.

6. Morton, B.R., Taylor, Sir Geoffrey and J.S. Turner, Turbulent Gravitational Convection From Maintained and Instantaneous Sources, Proc. Roy. Soc., vol. A234, pp. 1-23, (1956).

7. Stolzenbach, K.D. and D.R.F. Harleman, An Analytical and Experimental Investigation of Surface Discharges of Heated Water, Ralph M. Parsons Laboratory, M.I.T., Report No. 135, 1971.

8. Taylor, R.B. and R.G. Dean, Exchange Characteristics of Tidal Inlets, Proc. 14th Coastal Engineering Conference, pp. 2268-2289, 1974.

9. Ünlüata, Ü.A. and E. Özsoy, Nearshore Tidal Flows in the Vicinity of Inlets, Submitted to the J. Geophys. Res., February 1977.

10. Wang, J.D. and J.J. Connor, Mathematical Modeling of Near Coastal Circulation, Ralph M. Parsons Laboratory, M.I.T., Report No. 200, 1975.

11. Wright, L.D. and J.M. Coleman, Mississippi River Mouth Processes: Effluent Dynamics and Morphologic Development. J. Geology, vol. 82, pp. 751-778, 1974.

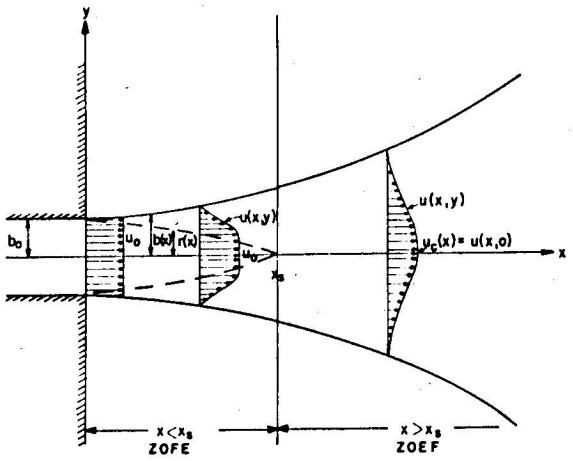

Figure I. Definition Sketch

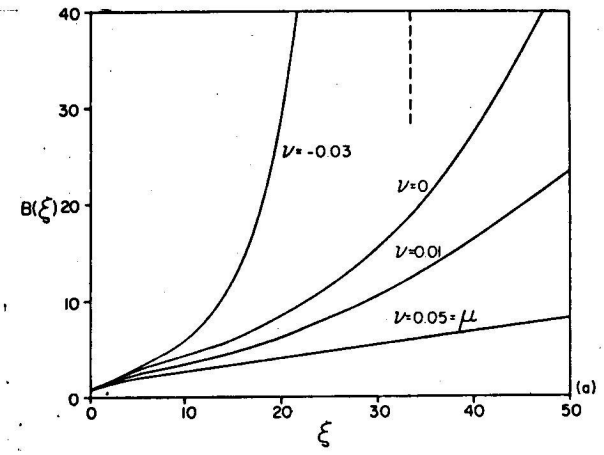

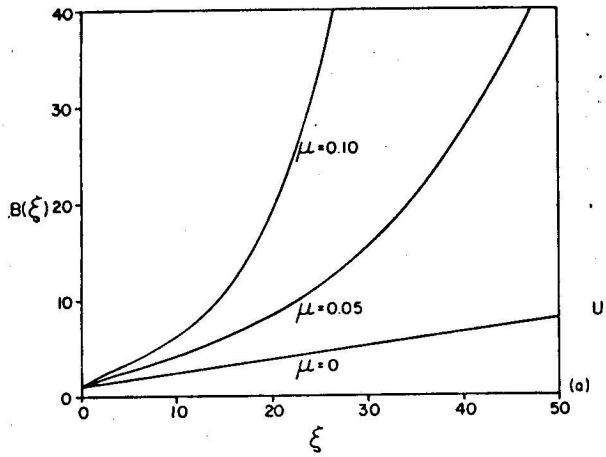

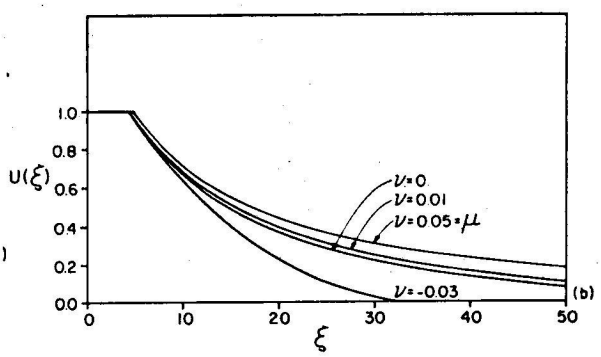

↑ Figure 3. Jet Characteristics Over a Linearly Varying Bottom, μ=0.05
(a) Jet Half - Width
(b) Centerline Velocity

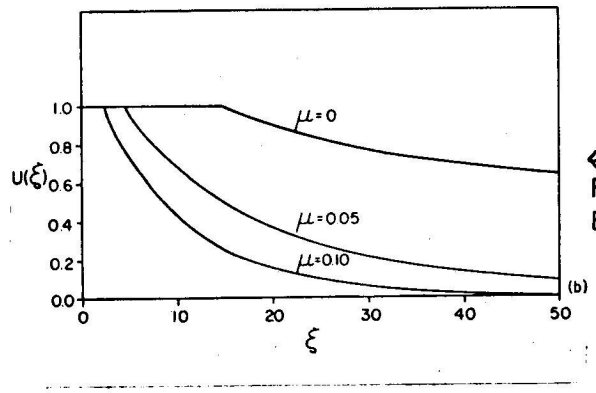

← Figure 2. Bottom Frictional Jet Over Constant Bottom (a) Jet Half-Width
(b) Centerline Velocity

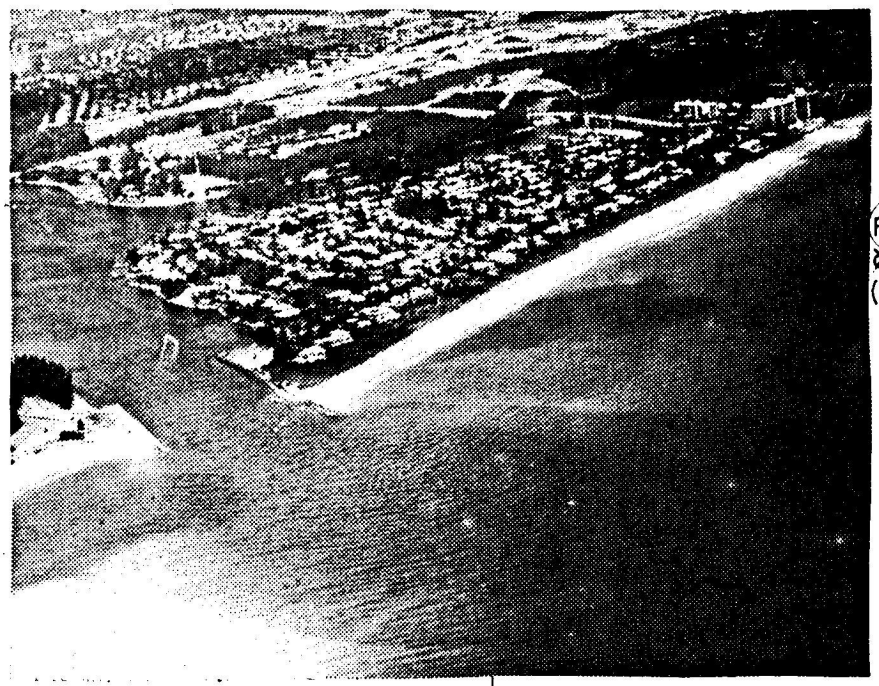

Figure 4. Jet Development at Jupiter Inlet, Florida (1973 Photograph)

Figure 5. Guide for Measuring Jet Width from Photograph in Fig. 4

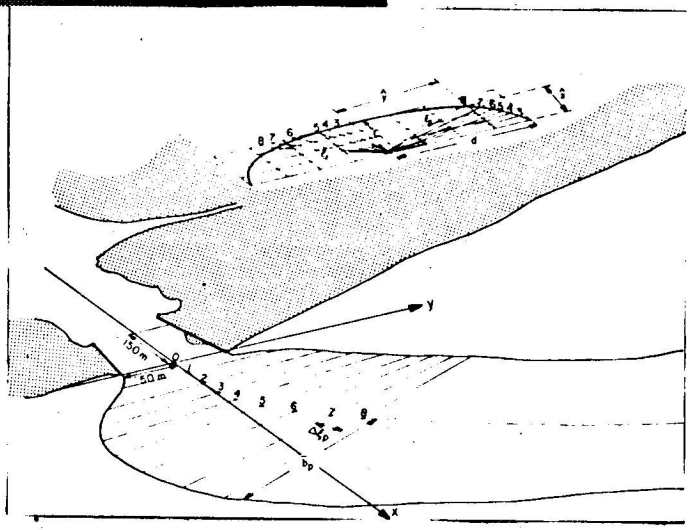

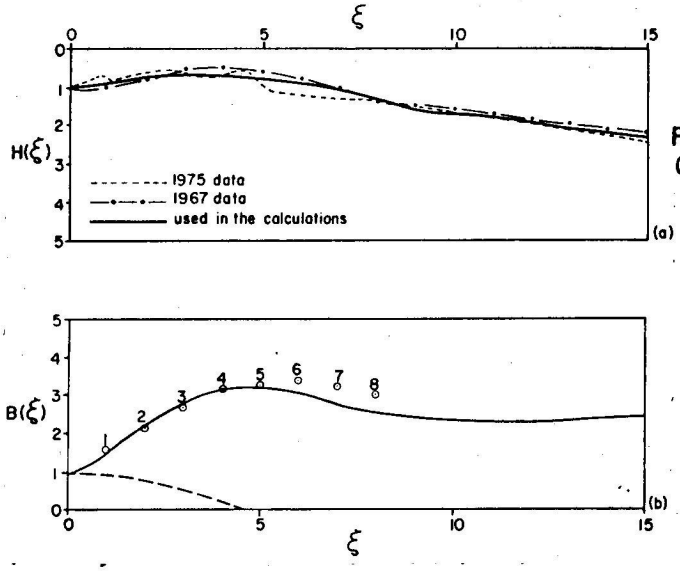

Figure 6. Comparison with the Jet Characteristics at Jupiter Inlet
(a) Depth Variations,
(b) Jet Half-Width, Measured (thick line) and Computed (points)

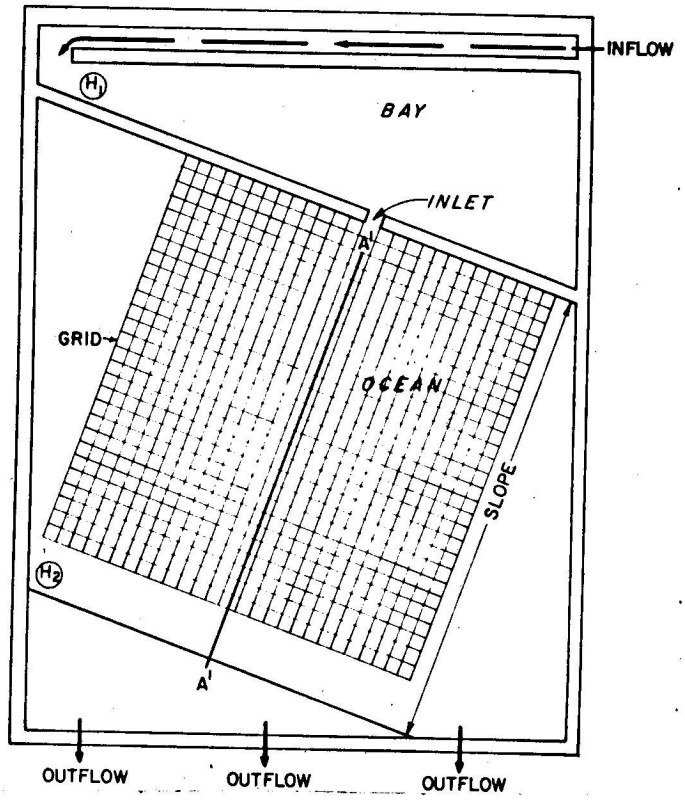

Figure 7. Model Basin Used in the Experiments

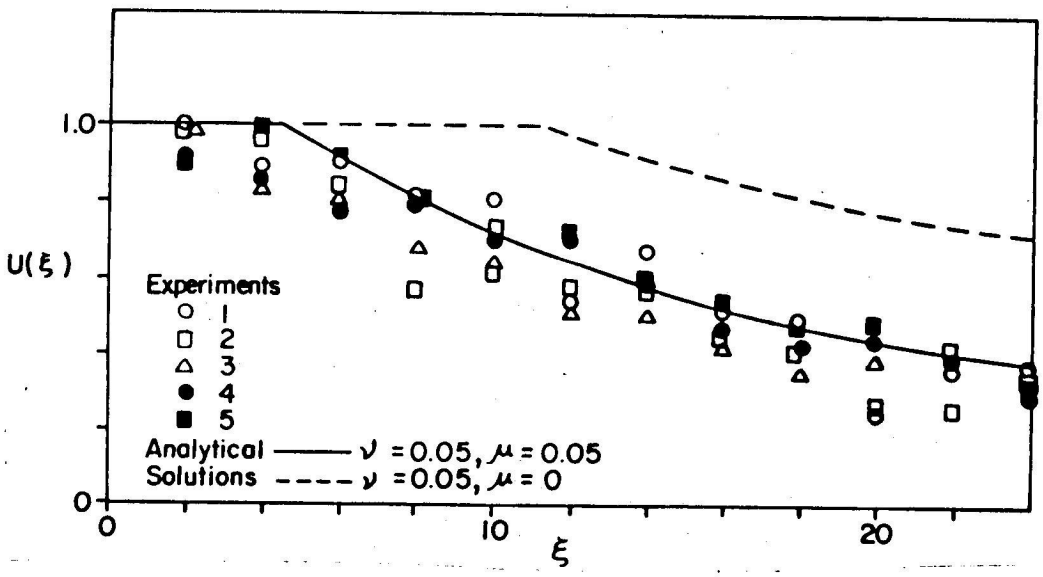

Figure 8. Comparison of the Analytical Solutions With the Experiments